Effective Electric Surface Susceptibility Tensor as a Probe of the Thermal Behavior of Langmuir−Blodgett Films

H. Hui-Litwin,[†] L. Servant,*[,‡] M. J. Dignam,[§] and M. Moskovits

Department of Chemistry, University of Toronto, 80 St. George Street, Toronto, Ontario M5S 1A1, Canada

Received: June 25, 1997; In Final Form: February 26, 1998

The thermal behavior of Langmuir−Blodgett (LB) monolayers of DL-dipalmitoyl phosphatidylethanolamine (DPPE) deposited onto a ZnSe substrate was studied by polarized infrared attenuated total reflection (ATR), over the temperature range 25−140 °C. The results are discussed in terms of the imaginary part of the effective electric susceptibility tensor [γ] of the monolayer, a function that approximately corrects for the effect of the local field. We show that the spectra of the imaginary parts of the principal components of [γ], Im(γ_t) and Im(γ_n) (the subscripts t and n representing the directions tangent to and normal to the film, respectively), can be straightforwardly obtained from polarized reflection spectra. The results obtained using Im(γ_t) and Im(γ_n) are compared with those obtained from the extinction coefficients k_t and k_n, which were calculated from adapted Kramers−Kronig relations. We show that Im(γ_t) and Im(γ_n) provide a better account of the molecular processes occurring in the DPPE LB films as a function of temperature. No abrupt phase transition was observed. This is attributed to positional disorder in the headgroups of the monolayer as it was initially transferred onto the ATR prism.

1. Introduction

Structural studies of Langmuir−Blodgett (LB) films at elevated temperatures are of great importance, as they provide information on the nature of phase changes in such layers. Additionally, these studies allow one to get insight regarding the poor stability of these films at elevated temperatures, which presently hinders their application, for example, in the field of electronics. It is therefore useful to develop efficient and simple methods for monitoring the structural changes that take place when LB films are heated. In principle, infrared spectroscopy provides information about the conformation of the molecules comprising the LB film and hence may be used to characterize some aspects of the molecular packing. In practice, the major problem in extracting information from spectroscopic data lies in the difficulties associated with defining a simple yet accurate model relating the dielectric response of an anisotropic monolayer to polarized radiation. It is well-known that typical LB films are composed of many small two-dimensionally ordered domains (size about 1 μm or smaller) with random azimuthal orientation. As a consequence, when modeling the optical reflection spectrum of a three-phase medium consisting of ambient/film/substrate, the LB films can be treated as a uniaxial layer with its optic axis normal to the monolayer substrate interface. Previously, we proposed a method for interpreting the polarized infrared reflection spectra for the study of LB films: instead of discussing the spectroscopic data in terms of, for example, the imaginary parts of the refractive indices (k_t, k_n),[1,2] we suggested treating them in terms of the imaginary parts of the principal elements of the effective surface electric susceptibility of the film: Im(γ_t) and Im(γ_n).[3,4] The main advantage of this approach lies in the fact that the spectra of Im(γ_t) and Im(γ_n) can be straightforwardly obtained from the polarized reflectance spectra and consequently do not require any mathematical processing of the data or additional information regarding the structure of the film, contrary to what is needed to obtain the spectra of k_t and k_n. Moreover, we showed that it was possible to relate Im(γ_t) and Im(γ_n) to some of the structural properties of the film such as the molecular packing and molecular orientation.

In the present study, we recorded the polarized ATR spectra as a function of temperature of LB monolayers of DPPE, and the spectra of the imaginary parts of the suceptibility tensor as well as the spectra of the imaginary parts of the refractive indices were extracted from the spectroscopic data. The paper is organized as follows: in section 2, we present the optical model and the origin of the effective electrical surface susceptibility, and we show how it is related to the reflectance spectra. In section 3, we describe how the films are prepared and the infrared spectra recorded. Finally, in section 4, we examine the influence of temperature on band profiles (intensity, width, and frequency) as deduced from the two approaches (surface effective electric susceptibility and extinction coefficients).

2. Optical Model of a LB Monolayer Lying on an Isotropic Substrate

Among the methods that have been developed to study films on various substrates, infrared reflection absorption techniques have been particularly successful. In this case, the spectrum is obtained by reflecting light from the [ambient/film/substrate] interface system, measuring the reflected intensity as a function of wavelength, and ratioing this signal with the reflected intensity from the uncovered surface obtained. The spectrum obtained in this way is a function of the wavelength λ_o and the

* To whom correspondence should be sent.

[†] Now at Centre for Infection and Biomaterials Research, The Toronto Hospital, Bell Wing, Ground Fl., Rm. 631, 200 Elizabeth St., Toronto, Ontario M5G 2C4, Canada.

[‡] Laboratoire de Physico-Chimie Moléculaire U.M.R. 5803 CNRS, Université Bordeaux I, 351, Cours de La Libération, 33405 Talence Cedex, France.

[§] Deceased.

S1089-5647(97)02084-1 CCC: $15.00
Published on Web 06/02/1998

state of polarization of the incident light, the angle of incidence, the thickness of the film, and the optical constants of the substrate, film, and ambient. Generally, it is assumed that the ambient phase and the substrate are treated as homogeneous, isotropic, and semi-infinite media and that the film, with a uniform thickness d, is homogeneous, uniaxial, and anisotropic, with its axis normal to the surface. In this case, it is then possible to express the reflection factor of such a three-phase medium as a function of the Fresnel coefficients of each interface (r_{jk} being the Fresnel coefficient of the interface j/k) and of the assumed thickness of the film. The optical properties of each phase j is specified by its complex index of refraction $n_j = m_j - ik_j$, where m_j is the real index of refraction and k_j the extinction coefficient. The reflectance of the three-phase stratified system with smooth, parallel, plane boundaries thus takes the standard form:[2,18]

$$r_\upsilon = \frac{r_{12}^\upsilon + r_{23}^\upsilon \exp(-ix^\upsilon)}{1 + r_{12}^\upsilon r_{23}^\upsilon \exp(-ix^\upsilon)} \qquad \upsilon = s, p \tag{1}$$

where υ = s or p according to whether the radiation is s or p polarized and x^υ is a complex quantity representing the change in phase of the light during one transversal of the adsorbate layer whose thickness is d:

$$x^\upsilon = 4\pi d n_{2t} \cos \phi^\upsilon / \lambda_o \tag{2}$$

In the case of thin films, one may question the relevance of considering planar and parallel boundaries between the layers, together with constant optical properties through the film. This is particularly true in the case of molecular layers such as LB films, formed from amphiphilic molecules with a hydrophilic "head" and a long hydrophobic "tail", whose dielectric tensor, if it can be defined at all for a thin film, must be a function of the distance from the film−substrate interface, the polarizability of the headgroup being different from that of the hydrocarbon tails. This problem was first raised by Drude in 1890.[19] More precisely, the characterization of an optical medium by phenomenological coefficients is only possible when the dimensions of the corresponding phases are large compared to the thickness of the boundaries layer to adjacent phases. In the case of monomolecular film, whose thickness is comparable with that of the boundary layer, this basic assumption does not hold, so that the dielectric tensor of the layer becomes dependent on its thickness.

Moskovits and Dignam[20,21] showed that this problem could be solved by introducing the so-called surface susceptibility tensor. These quantities are defined as

$$\gamma_t = (\epsilon_t/\epsilon_3 - 1)d \tag{3a}$$

$$\gamma_n = (1 - \epsilon_3/\epsilon_n)d \tag{3b}$$

and eliminates the quantities ϵ_t, ϵ_n, and d. In these relations, the subscripts 1 and 3 identify parameters related to the phases containing the incident and transmitted waves, respectively, and the dielectric functions of the film are represented by ϵ, with ϵ_n and ϵ_t being the principal dielectric tensor for the fields parallel to and transverse to the surface normal, respectively. Similarly, γ_t and γ_n are the normal and transverse elements of the effective surface electrical susceptibility tensor. Such quantities characterize the optical properties of the molecular layer through the relation

$$\tilde{\gamma}\mathbf{E_1} = 4\pi\mathbf{P_1} \tag{4}$$

where $\mathbf{E_1}$ is the electric field in the incident medium acting on the film and $\mathbf{P_1}$ is the medium effective induced dipole moment per unit area of the film. This follows directly from the definition of ϵ using appropriate boundary conditions in each case.[20] The strength of the surface susceptibility approach lies in the fact that in the case of thin films it provides a way of writing optical equations without using the film thickness. Thin films will be defined as in eq 1; exponential terms can be expanded as power series where terms of order 2 and higher can be neglected, i.e., $4\pi d n_t \cos\phi^\upsilon/\lambda_o \ll 1$. This inequality allows eq 1 to be linearized; after the appropriate algebra and substitutions, one obtains[2−5]

$$\ln(r_{\upsilon o}/r_\upsilon) = i2(\omega/c)\cos\theta_{in}[X_t + Y_\upsilon(X_t - X_n) - d] \tag{5}$$

where r_υ and $r_{\upsilon o}$ are the complex reflection coefficients for the film-covered and bare surface, respectively, ω is the angular frequency, c and θ_{in} are the speed of light and the angle of incidence in medium 1, respectively, and $i = \sqrt{-1}$. Note that d appears in the phase term and consequently cancels in the reflectivity. The remaining terms are defined as follows:

$$Y_p = \left[\cot^2\theta_{in} - \frac{\epsilon_1}{\epsilon_3}\right]^{-1}, \quad Y_s = 0 \tag{6a}$$

$$X_t = \frac{\gamma_t}{(\epsilon_1/\epsilon_3 - 1)}, \quad X_n = \frac{\gamma_n}{(1 - \epsilon_3/\epsilon_1)} \tag{6b}$$

Within an absorption band, γ_t and γ_n are complex valued, and from eq 5, one easily obtains

$$\mathrm{Im}(\gamma_t) = \left[\frac{(\epsilon_1/\epsilon_3 - 1)}{4(\omega/c)\cos\theta_{in}}\right][\ln(R_{so}/R_s)] \tag{7a}$$

$$\mathrm{Im}(\gamma_n) = \left[\frac{(1 - \epsilon_3/\epsilon_1)}{4(\omega/c)\cos\theta_{in}}\right][\ln(R_{so}/R_s)(1 + 1/Y_p) - \ln(R_{po}/R_p)/Y_p] \tag{7b}$$

where Im denotes the imaginary part and $R_{\upsilon o}$ and R_υ are the reflection factors for the bare and film-covered prism, respectively. The right-hand sides of eqs 5a,b depend on the dielectric constants of medium 1 and 3, the angle of incidence θ_{in}, and the polarized reflectance spectra, which are generally known. As a consequence, the spectra of $\mathrm{Im}(\gamma_t)$ and $\mathrm{Im}(\gamma_n)$ may be straightforwardly obtained from experimental data.

To relate these macroscopic observables to molecular properties of the film, an adequate model of the molecular film is required. Such a procedure was developed by Servant and Dignam,[3,4] who considered a LB film to be made up of randomly oriented biaxial domains, each of which is a regular two-dimensional array of point polarizable species. Provided that the monolayer contains only molecules of one species and that the local field corrections are supposed to be identical for each molecule, they were able to evaluate $\mathrm{Im}(\gamma_t)$ and $\mathrm{Im}(\gamma_n)$ analytically[3,4] as a function of molecular parameters such as the molecular polarizability and the array symmetry elements. They also introduced a dichroic ratio associated with an absorption band, $D_\gamma = \mathrm{Im}(\gamma_t)/\mathrm{Im}(\gamma_n)$, that they relate to the orientation of the corresponding transient dipole moment. In the case of a vibrational mode whose polarizability tensor is taken to be axially symmetric about the direction of the transition moment, it is possible to express D_γ for a transition dipole

moment tilted by an angle θ from the normal surface according to[3]

$$D_\gamma = \frac{\mathrm{Im}(\gamma_t)}{\mathrm{Im}(\gamma_n)} = G(a_1\alpha_\perp^0)\frac{1}{2}\tan^2\theta = \frac{1 + 3a_1\alpha_\perp^0 - 4(a_1\alpha_\perp^0)^3}{(1 - a_1\alpha_\perp^0)^3}\frac{1}{2}\tan^2\theta \quad (8)$$

In this expression, $G(a_1\alpha_\perp^0)$ is a function that takes into account the local field acting at a molecule, and the constant a_1, with dimensions of inverse volume, is a lattice sum of point dipoles taking into account the layer structure:

$$a_1 = \sum_i \frac{n_i}{2r_i^3} \quad (9)$$

In eq 9, n_i is the number of sites in the net at distance r_i from the central site. For a hexagonal net, $a_1 = 5.515/a^3$, where a is the nearest-neighbor separation. For very dilute films (a goes to infinity), a_1 tends to zero and the local field effect vanishes; otherwise, a_1 has a nonvanishing value that is related to the lattice constant of the hexagonal array. In eq 8, $\alpha_\perp^0$ is the high-frequency limit of the principal polarizability component, perpandicular to the transition dipole moment of the vibrational mode under investigation. An exact estimation of the polarizability tensor would require a complete quantum mechanical calaculation. However, a good estimate of $\alpha_\perp^0$ may be obtained for a given molecular group using the bond polarizabilities or molar refractivities,[6,22−24] which can be analyzed into contributions from the individual groups making up a molecule. Thus, bond refractivities are contributions that can be ascribed to bonds in covalent molecules. Such data have been tabulated for the Na D-line and are thus available in the required high-frequency limit. Nevertheless, recent progress in ab initio calculations suggests that accurate values of such polarizabilities for large molecules should soon become available. The lattice parameter a_1 characterizes the structure of the domains making up the film and depends on the nearest neighbor separation, which can be roughly estimated from pressure−area curves. Another way of estimating a_1 may rely on, for example, scanning tunneling microscopy (STM) or atomic force microscopy (AFM) images. Indeed, AFM and STM have been recently used to image LB films with molecular resolution.[25,26] The AFM in particular is extremely surface-sensitive, probing only the atoms located directly at the interface with lateral and vertical resolution smaller than 1 Å, and should be able to provide quantitative information on the molecular packing in LB films.[27] We think that this new approach, based on D_γ, is an improvement over the one based on the dichroic ratio involving the extinction coefficients $D_k = k_t/k_n = (1/2)\tan^2\theta$, because in the former, the local field acting on a molecule, its polarizability tensor, and its arrangement on the surface are explicitely considered, contrary to the one based on D_k, which models the film as a thin continuous and homogeneous layer, with a constant definite thickness d. Consequently, the surface susceptibility approach provides a connection between directly measurable quantities ($\mathrm{Im}(\gamma_t)$ and $\mathrm{Im}(\gamma_n)$) and the microscopic structure of the monolayer and its constituent molecules through their polarizability tensor and their surface arrangement (through a_1).

3. Materials and Methods

Materials. DL-DPPE ((Sigma, 98% purity), whose chemical structure is shown in Figure 1, was dissolved in 9:1:0.1 hexanes/methanol/chloroform to give a final concentration of 0.2 mg/mL and sonicated at 50 °C for at least 1 h prior to spreading. The solutions were kept in a freezer for storage for no longer than 3 months.

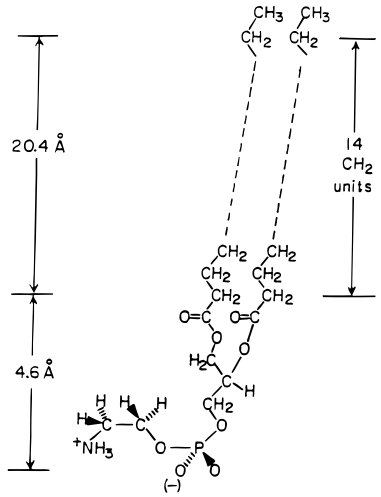

Figure 1. Structure of DPPE molecule.

A Lauda Film Balance (Sybron Brinkmann 1974) was used. Prior to each deposition, the trough was cleaned with ACS 2-propanol and methanol. The subphase was distilled deionized water with resistivity > 60 MΩ cm (IWT double cartridge system, Rolen Industries, Toronto, Ontario). After the trough was filled with the subphase, the pressure sensor was calibrated using the cross and weight set provided by Lauda. A monolayer was spread by applying 500−600 μL of solution dropwise to the water surface. Fifteen minutes were allowed for solvent evaporation, and the film was then compressed at 0.9 cm/min until the desired surface pressure was reached. The film was allowed to equilibrate an hour before deposition. Depositions were carried out with a Newport Linear Actuator 850 series, model PMC100, at approximatively 0.15 mm/s. The transfer ratio is 0.94 ± 0.04 at a surface pressure π = 30 mN/m. A spring-loaded frame with Teflon holding blocks secured the prism during deposition. After each run, the prism was cleaned by immersion in 3:1 $CHCl_3$/MeOH solution and sonicating for 3 h at 60 °C, and the solvent was changed every hour.

Infrared Measurements. Spectra were recorded with a resolution of 4 cm^{-1}, using a Bomem M110 upgraded to a MB100 with a mercury−cadmium−telluride detector. The sample chamber was purged overnight using a Balston air purification system, which removed CO_2 and water vapor. The ZnSe ATR prism was manufactured by Harrick Scientific Corp. A square prism was used in order to detect in-plane anisotropy: after the film was deposited, spectra obtained by rotating the prism through 90° were checked to be exactly superimposable onto the original spectra, establishing that the film was uniaxial. The edges of the prism are approximately 5.5 cm, its thickness is 3 mm, and the angle of incidence is 45°. The prism was held in a sample holder in the spectrometer during scanning. The holder consisted of two copper slabs, with the prism sandwiched between them. The inside surfaces of the holder were coated with a gold layer (Applied Physics, Toronto, Canada). The cell was built such that thermal contact was made only at its outer perimeter. To raise the LB monolayers to elevated temperatures, heating cartridges were inserted into the prism holder (two cartridges for each block) and controlled by Omega temperature controllers (model CN9000A).

The rate of heating was 0.67 °C/min, and the sample was heated from 25 °C to a maximum of 140 °C. The heater was

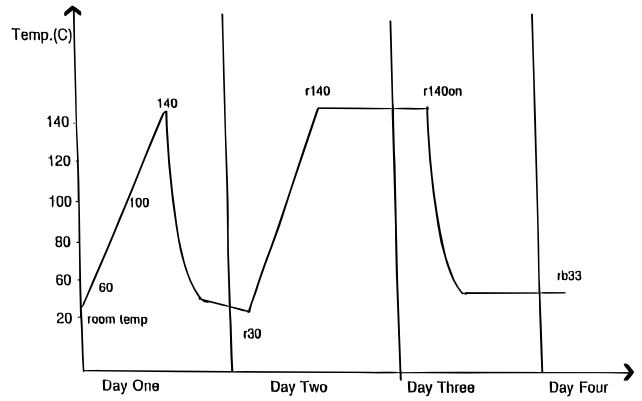

Figure 2. Stages of heating and cooling in thermal studies of DPPE monolayers.

then shut off, and the film was allowed to cool overnight. After the film was annealed the next day, it was reheated to 140 °C and allowed to equilibrate overnight at that temperature. The following day, another scan was taken of the film at 140 °C before allowing it to cool again to room temperature. A final scan was taken on the next day, before removing the film from the prism. The various stages of heating and cooling are summarized in Figure 2.

4. Results and Discussion

The s- and p-polarized ATR infrared spectra of the bare prism were measured first, at ambient temperatures, and were kept as reference for subsequent measurements. Both s- and p-polarized ATR infrared spectra of the DPPE-monolayer-covered surface were measured at various temperatures, and the change in reflectivity $R_{\upsilon o}/R_{\upsilon}$ was obtained by taking the ratio of the spectrum obtained from the bare prism to that obtained from the monolayer-covered prism. Finally, the spectra of the susceptibility elements, Im(γ_t) and Im(γ_n), were obtained using eqs 7a,b. The spectra of k_t and k_n were calculated using the method of Bardwell and Dignam,[1,2] who developed an approach based on an extension of the Kramers−Kronig transformation, which provided the spectra of the optical constants of a sample from its ATR spectra. To do so, the thickness of the film under consideration was assumed to be $d = 0.0025$ μm and the high-frequency limit of the refractive index, whose knowledge is necessary for the computing of the data, was taken to be $n = 1.5$.

The CH_2 stretching mode region of the spectra is shown as a function of temperature in Figures 3 and 4. This spectral region is dominated by two strong bands at 2920 and 2850 cm^{-1}, assigned to the methylene antisymmetric and symmetric stretching modes, respectively.[6,7] Weaker bands due to the asymmetric and symmetric stretching modes of the terminal methyl group are also observed (for p polarization) near 2950 and 2870 cm^{-1},[8,9] respectively. As the temperature increases, the two methylene bands exhibit the same behavior for both (Im(γ_t), Im(γ_n)) and (k_t, k_n): they become broader and shift to higher frequencies. Earlier studies have ascribed the bandwidth increase to an increase in the rotational mobility of the acyl chains and the frequency shift to the introduction of gauche conformers in the acyl chains at high temperatures.[15] The CH_3 symmetric stretch band at 2875 cm^{-1}, which can be seen clearly in the spectra of the normal component, weakens with increasing temperature. This suggests that as the chains melt, the methyl ends of the chains adopt a more random orientation, so that the methyl groups are no longer aligned with their axes oriented close to the normal.

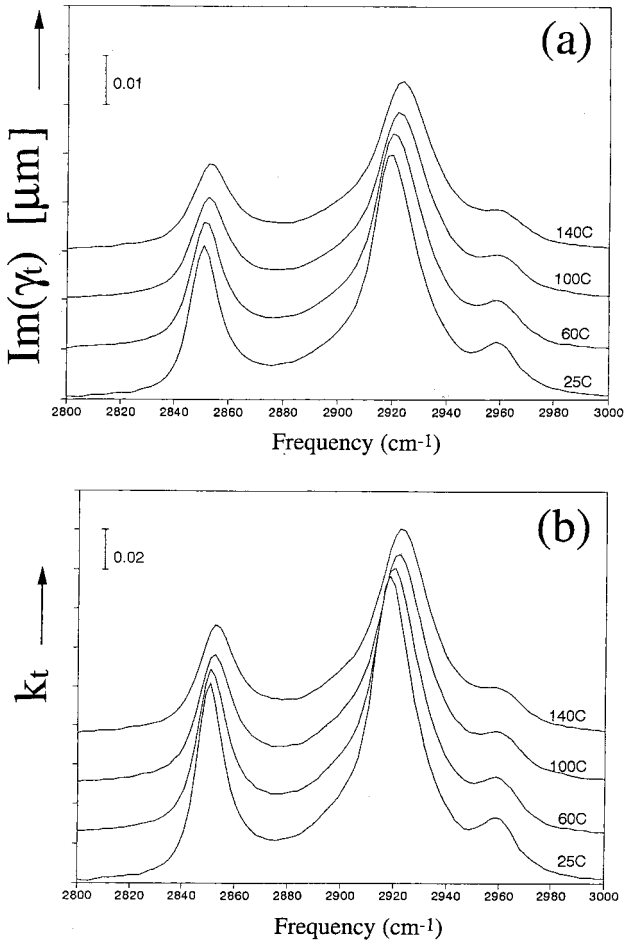

Figure 3. Plots of Im(γ_t) (a) and of k_t (b) for a DPPE monolayer in the CH stretching mode region, as sample is being heated.

The spectral region ranging from 900 to 1100 cm^{-1} displayed in Figures 5 and 6, for both (Im(γ_t), Im(γ_n)) and (k_t, k_n), contains two sets of broad bands, which correspond mainly to vibrations of the headgroups. The PO_2 asymmetric stretch is a broad band at 1225 cm^{-1}, while the PO_2 symmetric stretch is at 1080 cm^{-1}. These bands overlap with several other bands, such as the CH_2 wagging vibration bands, characteristic of an all-trans methylene chain conformation, and also with other bands, of uncertain assignment, which likely belong to vibrations of C−O and CCN. The group of bands between 1000 and 1300 cm^{-1} broadens above 100 °C. The higher frequency component at 1225 cm^{-1} loses intensity, and the overall group becomes more rounded in shape.

The temperture dependence of the band-center frequencies of the CH_2 asymmetric and C═O stretching modes are presented in Figure 7. The center frequencies of the normal and transverse components of the bands are different in both the Im(γ) and the k spectra. These frequency differences are due to several effects. Because band-center frequency differences obtained from γ (ω(Im(γ_n)) − ω(Im(γ_t))) are significantly smaller than those obtained from the spectra of the absorption index (ω(k_n) − ω(k_t)), some of the n to t frequency shift in the k_n and k_t spectra is clearly associated with the local field. The frequency difference (ω(Im(γ_n)) − ω(Im(γ_t))) associated with the CO stretching vibration mode ranges from 0.2 to 1.3 cm^{-1}, as compared to 3.3 to 4.3 cm^{-1} in the corresponding k spectra. For CH_2 asymmetric stretching bands, the frequency difference (ω(Im(γ_n)) − ω(Im(γ_t))) is approximately 2.6 cm^{-1}, slightly higher than what is observed for CO bands, but smaller than the corresponding frequency differences of approximately 5.5

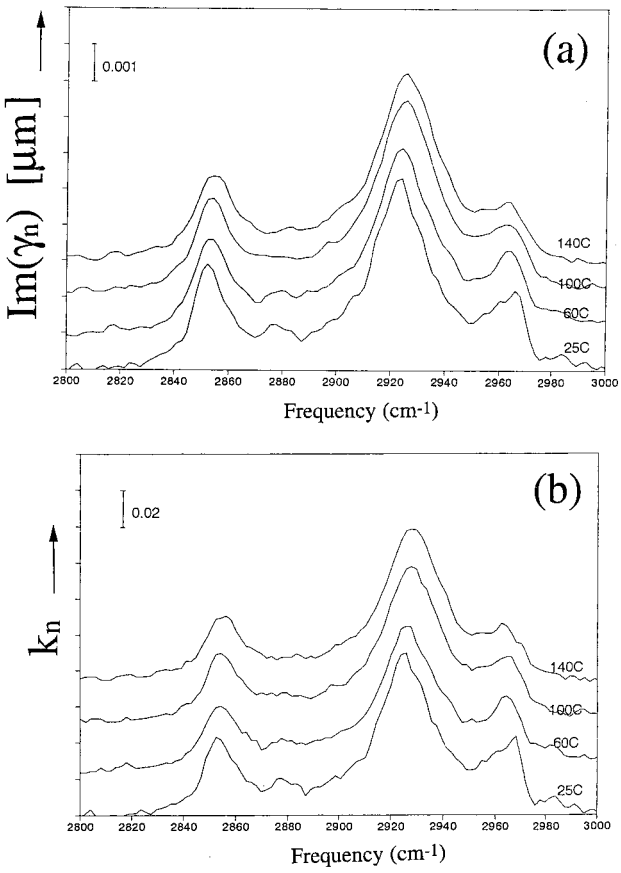

Figure 4. Plots of Im(γ_n) (a) and of k_n (b) for a DPPE monolayer in the CH stretching mode region, as sample is being heated.

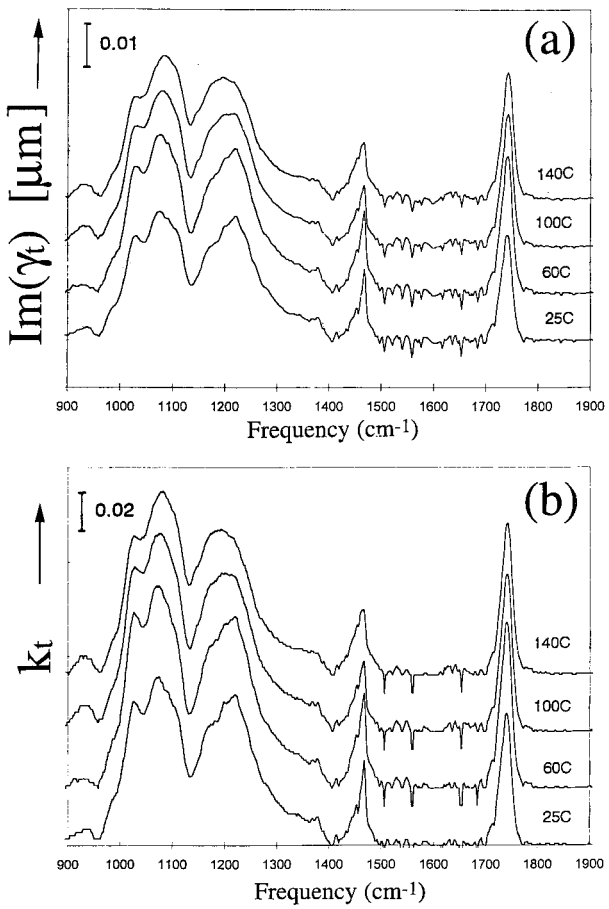

Figure 5. Plots of Im(γ_t) (a) and of k_t (b) for a DPPE monolayer in the headgroup region, as sample is being heated.

cm^{-1} observed in the *k* spectra. The theoretical analysis[2−5] of the effective electrical surface susceptibility corrects for the frequency shifts observed in s- and p-polarized spectra brought about entirely as a result of the neglect of the influence of the local field, and indeed, the experimental results show that the (ω(Im(γ_n)) − ω(Im(γ_t)) differences are systematically smaller than those in the corresponding *k*. This is demonstrated most dramatically for the CO stretching mode, which is a particularly good candidate for testing this model since it most closely fulfills our assumption of a planar array of oscillating dipoles.

On cooling the film from 140 °C, the band-center frequencies decrease, suggesting that the number of trans conformers in the sample increases as the monolayer is cooled (see Figure 8, r30). However, the band frequencies do not decrease to their original values, indicating that the order of the chains is only partially recovered. Further heating (Figure 8 at points marked "r140" and "r140on") causes the frequency of these bands to shift to higher wavenumbers again, which is consistent with an increasing number of gauche conformers resulting from repeated heating. After the final cooling cycle (rb30), the frequency remains higher than both that of the original film and that of the film after its first heating, indicating that the overall disorder of the film increases with the number of heating cycles. This is in agreement with what was found for cadmium arachidate LB multilayers,[10] where "residual disorder" remains in the film after repeated heating cycles. This "frozen in" disorder is not unusual; disorder can be induced rapidly since it requires only local motion, while order takes longer to establish. Its delocalized nature increases the apparent activation barriers encountered in achieving order.

We now consider the average conformation of the DPPE molecule within the film at room temperature. To do so, we employ the model described in section 2, and the angles are specified in Figure 9. The bands were curve fitted using the Labcalc software (Galactic). The CH stretching mode was fitted with Lorentzians, which gave a better fit visually than Gaussians. The following parameter values were used in the model. A hexagonal packing of the molecules was assumed within a given domain; hence $a_1 = 5.515/a^3$, where *a* is the nearest neighbor distance. For the CH_2 and CO groups, the distance *a* is estimated to be 4.6 Å for close packed chains. This value is taken from X-ray crystal data for DPPE single crystals,[12] and a_1 is thus equal to 0.049 87 $Å^{-3}$. As mentioned above, a better estimate might be provided from AFM or STM images. An estimate of $\alpha_\perp^0$, the high-frequency polarizability of the vibrating group considered (i.e., CH_2 and CO groups), was obtained using molar refractivities. The molar refractivities can be obtained, to a fair approximation, from contributions from individual groups making up a molecule. Thus, bond refractivities can be ascribed to individual covalent bonds. The bond refractivity, *R*, for CH bond is approximately 1.69 cm^3.[6] Therefore, *R* for the CH_2 group is approximatively 2(1.69)cm^3 = 3.38 cm^3. Substituting this value into eq 7, one obtains $\alpha_\perp^0$ = 1.34 $Å^3$, which, together with a_1 = 0.049 86 $Å^{-3}$, produces $G(a_1\alpha_\perp^0) = G$ = 1.48 (eq 6). For the CH_2 asymmetric stretch at room temperature, one obtains D_γ = 14.73. Substituting D_γ and *G* values into eq 6, one obtains θ_{asym} = 74° as the angle of the CH_2 asymmetric stretch dipole tilt from the *z* axis at 25 °C. Similarly, one calculates the angle of the dipole of the CH_2 symmetric stretch to be θ_{sym} = 75°. A relationship exists between the tilt angle of an hydrocarbon chain, θ, and those of the transition dipoles associated with the

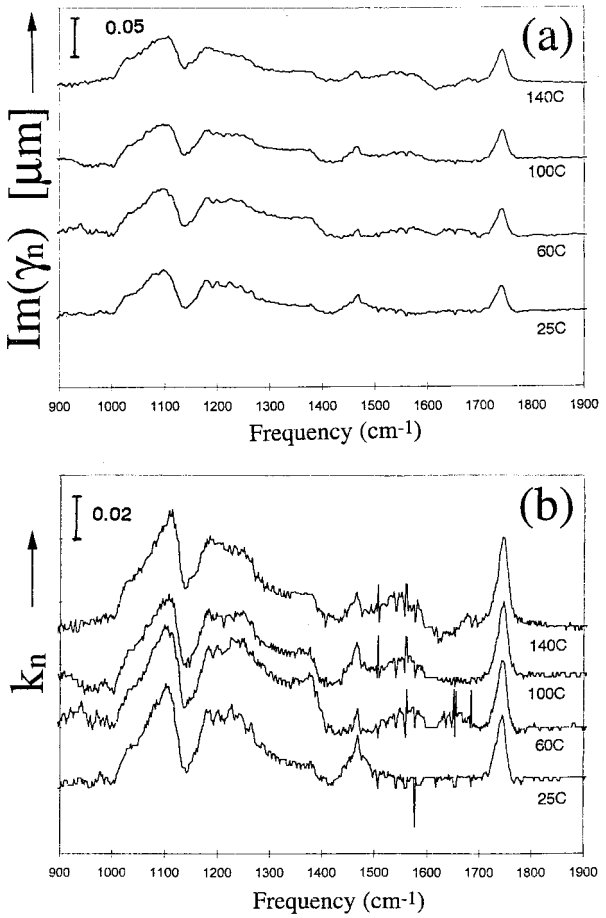

Figure 6. Plots of $\mathrm{Im}(\gamma_n)$ (a) and of k_n (b) for a DPPE monolayer in the headgroup region, as sample is being heated.

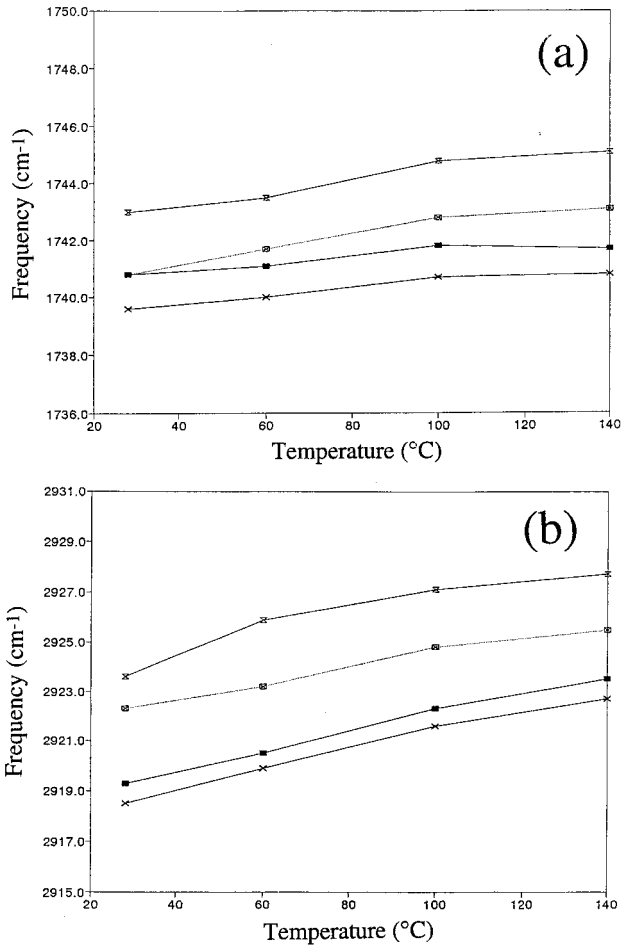

Figure 7. Plots of the band frequencies $\omega(k_x)$ and $\omega(\mathrm{Im}(\gamma_x))$, where x = t, n, as a function of temperature, (a) for the CO stretching mode, and (b) for the CH_2 asymmetric stretching mode: × = $\omega(k_t)$, ⧖ = $\omega(k_n)$, ⊞ = $\omega(\mathrm{Im}(\gamma_n))$, ■ = $\omega(\mathrm{Im}(\gamma_t))$.

CH_2 asymmetric (θ_{asym}) and symmetric (θ_{sym}) modes:[11]

$$\cos^2\theta_{asym} + \cos^2\theta_{sym} + \cos^2\theta = 1 \qquad (10)$$

from which one can calculate the chain tilt angle to be $\theta = 22°$. Using D_k, one obtains a larger angle, $\theta = 37°$. Furthermore, it has to be noted that the value obtained for θ from D_γ is consistent with the one obtained by Akutsu et al.,[28] who found, using infrared dichroism, that hydrocarbon chains are inclined at an angle of 25° to the film normal, in the case of built-up films of DPPE.

As temperature rises, it becomes more and more difficult to characterize unambiguously the tilt angle of the hydrocarbon chains using eq 10, due to the incorporation of trans−gauche sequences. Such characterization would be valid if one assumes the presence of only a few gauche bonds, located close to the top of the chain, and would provide an average measure of the tilt angle of the carbon chain. X-ray diffraction studies have shown[12] that disorder in the chain begins at the methyl ends, which suggests that gauche conformers may be localized primarily near the methyl ends of chains, a view that is supported in the present case by the disappearance of the normal component of the methyl symmetric stretch when temperature augments.

The behavior of the peak frequency as a function of temperature suggests that the deposited PE monolayer did not go through a sudden phase transition but, rather, becomes disordered gradually with increasing temperature. This is in contrast with the behavior of DPPE aqueous dispersions[15] and with other LB films. Naselli et al.[17] observed a sharp phase transition in cadmium arachidate multilayers and suggested that it was due to a breakup in the headgroup lattice, when multilayers are heated above 120 °C, leading to irreversible disorder. However, the X-ray diffraction studies of Tenchov et al.[15] showed that disruption of the H-bonding network within the headgroup due to hydration causes the transition to have less than first-order character. Therefore, the absence of a sudden phase transition for LB monolayers of PE might be due to the fact that the headgroups in the deposited monolayer were never in a regular lattice, even when freshly deposited. Although the headgroups are linked in a H-bonded network between PE molecules in single crystals,[12] this network may only be partially present in a PE monolayer spread on the water surface. This is because the headgroups now have the opportunity to H-bond with the water molecules of the subphase in addition to neighboring headgroups. As a result, the headgroups in the monolayer at the air/water interface probably adopt a variety of orientations, as was found in a molecular dynamical simulation study of the PE/water system.[16] Transfer of this monolayer onto the ZnSe substrate might have retained this inherent disorder of the headgroups. Furthermore, comparison of the headgroup region of our monolayer with IR transmission spectra of solid, crystalline PE at various temperatures showed that the headgroups were indeed disordered even at room temperature. At 25 °C, the headgroup region (900−1400 cm^{-1}) of the solid-state PE spectrum is made of sharp bands.[14] These are seen to broaden and merge until only a few broad bands remain at 120 °C. The LB monolayer spectra of

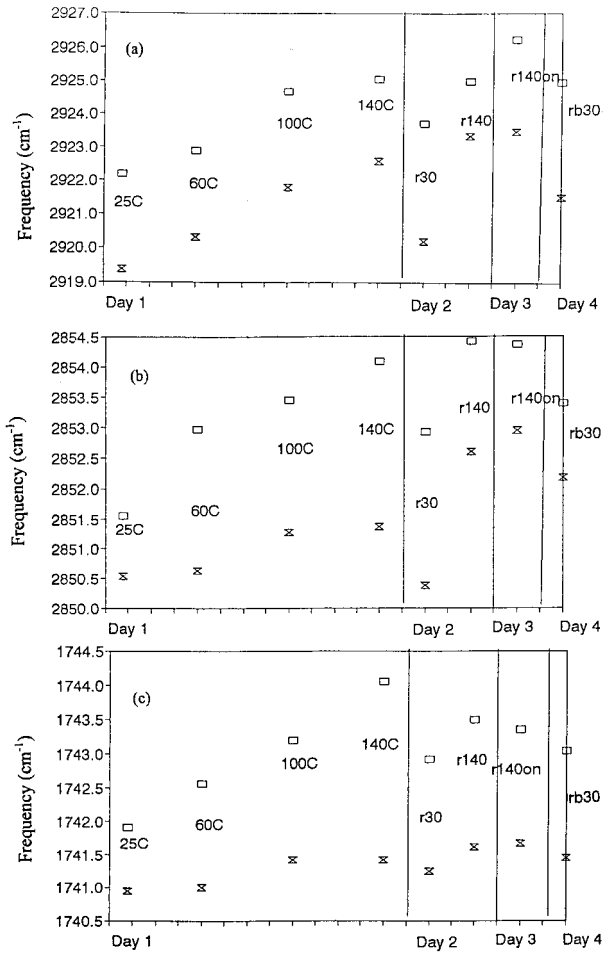

Figure 8. Plots of frequency maxima of $\omega(\mathrm{Im}(\gamma_t))$ (⊠) and $\omega(\mathrm{Im}(\gamma_n))$ (□) for various modes, as a function of temperature, during the various stages of the heating cycle: (a) CH_2 asymmetric stretch; (b) CH_2 symmetric stretch; (c) C═O stretch.

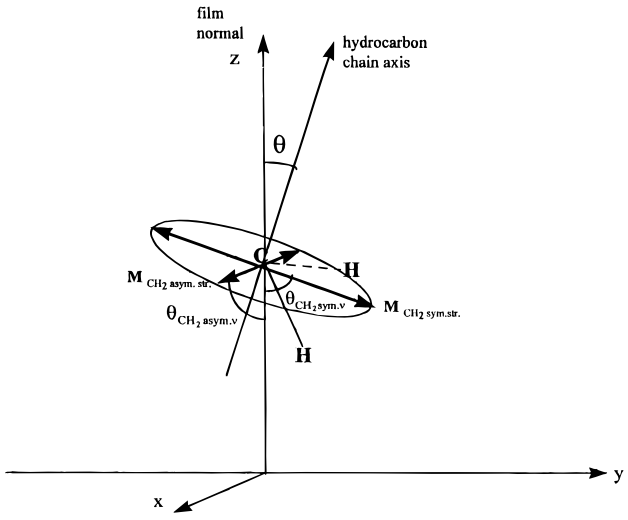

Figure 9. Angles and coordinate system used to describe the conformation of the hydrocarbon chains (M stands for the transition dipole moments).

the headgroup region at room temperature, in fact, resembles the PE spectra at 120 °C, suggesting that the headgroups are not in a crystalline form even at room temperature. Therefore, in LB monolayers of DPPE, the chains melt gradually with temperature, similar to what occurs in LB multilayers of cadmium arachidate and TCNQ. However, unlike those LB multilayers, the monolayer does not have a sudden phase transition, due to the absence of an ordered headgroup lattice.

5. Conclusion

DPPE monolayers deposited onto ZnSe were studied as a function of temperature, using polarized ATR spectroscopy. A critical issue with regard to the study of infrared spectra of LB films is the choice of an appropriate structural model describing the film itself and its relation with the spectroscopic observables. On the basis of rigorous studies of LB films by STM and AFM, it is clear that considering such thin films as homogeneous phases with smooth, parallel, and plane boundaries is only an approximation. The present study demonstrated that significant information regarding the microscopic structure of the film can be straightforwardly obtained from spectroscopic data by using the normal and tangential components of the electric susceptibility data, without any assumption on film thickness (except it is thin). This new approach also provides a more realistic description of the film structure to be assumed rather than assuming the film to be a continuous layer. This allows one to study the molecular conformation of transition dipole moments associated with individual vibrations, incorporating details on the film structure through the a_1 constant, in the case of a film of hexagonal symmetry. We showed by monitoring the antisymmetric and symmetric CH_2 stretching bands that as the monolayer is heated to 140 °C, disorder increases continuously and appears to be mainly localized near the end hydrocarbon tail methyl groups. The absence of an abrupt phase transition is likely due to positional disorder in the headgroups in the monolayer as it is initially transferred to the prism.

Finally, from a more general point of view, our goal was to explore the spectroscopic properties of LB films from a different perspective than the one usually adopted. We believe that these experiments pave the way for future studies, as they have shown that the susceptibility tensor is quite sensitive to the temperature-induced modifications experienced by a LB film. Work remains to be done to develop further the film molecular model and to analyze more accurately the influence of various parameters (molecular area and its possible variations, high-frequency limit of the polarizability tensor, etc.) on band profiles in order to be able to obtain insight on the molecular structure of LB films from spectroscopy.

Acknowledgment. We wish to thank NSERC and CEMAID for financial support. We are grateful to S. Mamiche-Afara for helping with the experiments and proofreading the manuscript.

References and Notes

(1) Bardwell, J.; Dignam, M. J. *J. Colloid Interface Sci.* **1987**, *116*, 1.
(2) Bardwell, J.; Dignam, M. J. In *Fourier Transform Infrared Characterization of Polymers*; Ishida, H., Ed.; Plenum Publishing Corp.: New York, 1987.
(3) Servant, L.; Dignam, M. J. *Thin Solid Films* **1994**, *242*, 21.
(4) Servant, L.; Dignam, M. J. To be published.
(5) Dignam, M. J.; Moskovits, M.; Stobie, R. W. *Trans. Faraday Soc.* **1971**, *67*, 3306.
(6) Denbigh, K. *Trans. Faraday Soc.* **1940**, *36*, 936.
(7) Asher, I. M.; Levin, I. W. *Biochim. Biophys. Acta* **1977**, *63*, 468.
(8) Cameron, D. G.; Casal, H. L.; Mantsch, H. H. *Biochemistry* **1980**, *19*, 3665.
(9) Fringelli, U. P.; Gunthard, H. H. *Membrane Spectroscopy*; Springer-Verlag: New York, 1981; p 270.
(10) Casal, H. L.; Mantsch, H. H. *Biochim. Biophys. Acta* **1984**, *779*, 381.
(11) Hasegawa, T.; Takeda, S.; Kawaguchi, A.; Umemura, J. *Langmuir* **1995**, *11*, 1236.
(12) Elder, M. *Proc. R. Soc. London, A* **1977**, *354*, 157.

(13) Tenchov, B.; Lis, L.; Quinn, P. *Biochim. Biophys. Acta* **1988**, *942*, 305.
(14) Chapman, D.; Byrne, P.; Shipley, G. G. *Proc. R. Soc. London, A* **1965**, *390*, 115.
(15) Lafrance, D.; Marion, D.; Pezolet, M. *Biochemistry* **1990**, *29*, 4592.
(16) Raghavan, D. K.; Reddy, M.; Berkowitz, M. *Langmuir* **1992**, *8*, 233.
(17) Naselli, J.; Rabolt, F.; Swallen J. D. *J. Chem. Phys.* **1985**, *82*, 2136.
(18) Heavens, O. S. *Optical Properties of Thin Solid Films*; Dover: New York, 1965.
(19) Drude, P. *Ann. Phys.* **1890**, *39*, 504.
(20) Dignam, M. J.; Moskovits, M. *J. Chem. Soc., Faraday Trans. 2* **1973**, *69*, 65.
(21) Dignam, M. J.; Moscovits, M. *J. Chem. Soc., Faraday Trans. 2* **1973**, *69*, 56.
(22) Bottcher, C. J. F.; Van Belle, O. C.; Bordewijk, P.; Rip, A. *The Theory of Electric Polarization*; Elsevier: New York, 1973.
(23) Huang, W. T.; Levitt, D. G. *Biophys. J.* **1977**, *17*, 111.
(24) Smith, R. P.; Mortensen, E. M. *J. Chem. Phys.* **1960**, *32*, 502.
(25) Bourdieu, L.; Silberzan, P.; Chatenay, D. *Phys. Rev. Lett.* **1991**, *67*, 2029.
(26) Garnaes, J.; Schwartz, D. K.; Viswanathan, R.; Zasadzinski, J. A. N. *Nature* **1992**, *357*, 54.
(27) Schwartz, D. K.; Garnaes, J.; Viswanathan, R.; Chiruvolu, S.; Zasadzinski, J. A. N. *Phys. Rev. E* **1993**, *47*, 452.
(28) Akutsu, H. Kyogoku, Y.; Nakahara, H.; Fukuda, K. *Chem. Phys, Lipids* **1975**, *222*, 15.